FLOW THROUGH A PLANE ORIFICE IN A PIPE WALL

BY
J.A. SANDOVER *
AND
J.A. TALLIS **

Theoretical analysis

(*a*) A SINGLE ORIFICE WITH THE PIPE OUTLET DISCHARGING TO ATMOSPHERE, Figure 1.

Let the discharge through the orifice :

$$q = aC_D\sqrt{2\,p/\rho} \qquad (1)$$

where C_D is a discharge coefficient, p is the mean value of p_1 and p_2 and ρ is the fluid density. Further, since the discharge at section 3 is to atmosphere,

$$p_2 = 2\,c_f\frac{L}{D}\rho u^2\ (*) \qquad (2)$$

and if the Reynold's Number for the flow, $\mathcal{R}$, is less than 10^5 the friction coefficient,

$$c_f = 0.079\,\mathcal{R}^{-1/4} \qquad (3)$$

Substituting 2 and 3 in 1 and assuming $p = p_2$

$$q = 0.443\,C_D d^2 u^{7/8} L^{1/2}\nu^{1/8}/D^{5/8} \qquad (4)$$

where $\nu\,(=\mu/\rho)$ is the kinematic viscosity of the fluid.

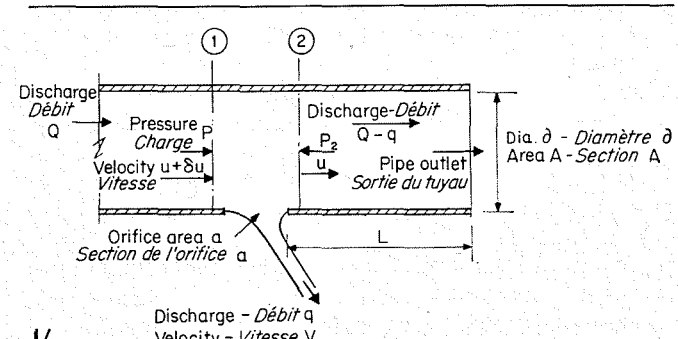

1/

Then for steady conditions,

$$q = K_1 u^{7/8}\ (*) \qquad (5)$$

and K_1 has to be determine experimentally.

Further applying the momentum equation to a control surface coinciding with the pipe walls, section 1 and section 2;

$$(p_1 - p_2)\,A = \rho u^2 A - \rho\,(u + \delta u)^2 A \qquad (6)$$

* Ph. D.
** B. Sc.

(*) This is not entirely correct as will be shown in the section on Head and Pressure variations. However it would be extremely difficult to provide analytically for the additional pressure gradient which is due to breakway and turbulence.

or

$$p_1 - p_2 = -2\rho u \delta u \tag{7}$$

if second order terms are neglected. This expression implies that a pressure *rise* occurs across the orifice.

A form of the continuity equation is

$$q = A\delta u \tag{8}$$

Using this and equation 4, equation 7 reduces to

$$p_2 - p_1 = 1.128\ C_v d^2 u^{15/8} L^{1/2} \nu^{1/8} / D^{21/8} \tag{9}$$

$$= K_2 u^{15/8} \tag{10}$$

if the conditions are steady.

If the flow is laminar, $c_f = 16\ \mathcal{R}$ and

$$q = 8\ C_D \frac{a}{D} \left(\frac{\mu u L}{\rho} \right)^{1/2} \tag{11}$$

$$= K_3 u^{1/2} \tag{12}$$

Further,

$$p_2 - p_1 = 20.38\ C_v \frac{a u^{3/2}}{D^3} (\rho u L)^{1/2} \tag{13}$$

$$= K_4 u^{3/2} \tag{14}$$

VARIATION IN PRESSURE AND TOTAL ENERGY IN A TEST LENGTH:

Considering a test length l on either side of an orifice, the total energy loss over the length $2l$ can be expressed as the sum of the individual losses. These comprise; the normal friction loss in the upstream length l (where the mean velocity is $(u - \delta u)$, the kinetic energy loss due to leakage, the apparent energy gain due to the pressure rise across the orifice, the normal friction loss in the downstream length where the mean velocity is u and an *excess* energy loss in this length.

This excess energy loss is represented by Δ_{pe} in Figure 2. This is a diagram showing the variation in pressure with distance. Curve A is the normal Fanning loss, B the orifice pressure rise and C would represent the continued Fanning fall. In practice the actual pressure drop follows some curve such as D which ends a distance below C represented by Δ_{pe} the excess energy loss. The curve D however is always above the curve E which is a continuation of A and represent the normal Fanning loss. Therefore when the experiment were originally carried out this reduction in pressure loss over the length $2l$ gave rise to considerable speculation particularly as it did not correspond to the pressure rise across the orifice.

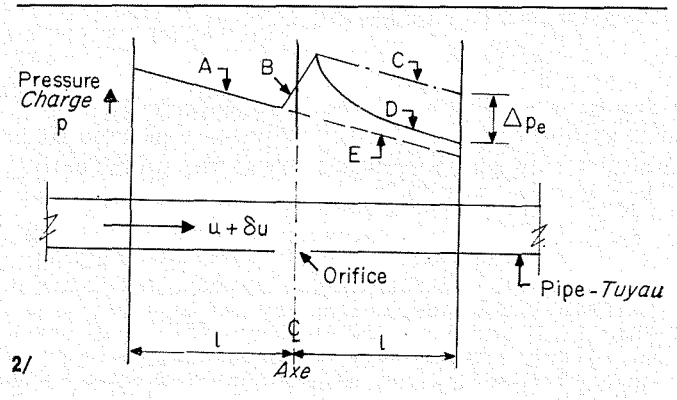

2/

The total energy loss can be expressed after some manipulation as

$$\Sigma \Delta H = \frac{2 c_f \rho l}{D} \frac{Q^3}{A^2} + \rho q \left\{ \frac{q^2}{2 C_D^2 a^2} - \frac{2}{A^2} (Q^2 - Qq) \right\} + \frac{2 c'_f \rho}{D} A u l \int_0^l f(u, l)\, dl. \tag{15}$$

where the final term represents the excess energy loss in the downstream length l and c'_f is a coefficient (similar to c_f) which is supposed to depend upon the Reynold's number of the flow and $f(u, l)$ is some function of velocity and distance. This expression needs considerable investigation. Further

$$\Sigma \Delta H = \left\{ \frac{P_u}{\rho g} + \frac{(u + \delta u)^2}{2g} \right\} \rho g A (u + \delta u) - \left\{ \frac{P_d}{\rho g} + \frac{u^2}{2g} \right\} \rho g A u \tag{16}$$

where the suffices u and d refer to the upstream and downstream limits, respectively, of the length $2l$. From the equations 13 and 16 it is therefore possible to investigate the excess friction term further.

The pressure loss in the test length will be composed of:—

$$\Sigma \Delta p = 2 c_f \rho \frac{l}{D} (u + \delta u)^2 + 2 c_f \rho \frac{l}{D} (u^2) - 2 \rho u \delta u + 2 c'_f \rho \frac{l}{D} \int_0^l f(u, l)\, dl \tag{17}$$

$$= 2\rho \left\{ c_f \frac{l}{D} (u^2 + u\delta u) - u\delta u + c'_f \frac{l}{D} \int_0^l f(u, l)\, dl \right\} \tag{18}$$

In the experiments each of these terms in known except the final one which can therefore be determined.

More than one orifice and the pipe exhausts to atmosphere

Since the pipe may run full or part-full downstream and the flow may be laminar or turbulent it is possible to have a number of flow combinations. However, only turbulent flow with the pipe running full will be considered. Further, although the pressure drop and the energy losses can be predicted using the theory developed above, experimental evidence indicates that breakaway and excess turbulence downstream of an orifice produce effects which most certainly are not in accordance with any simple theory. A description of these experiments is included in the next section with an indication of the anomalies that can occur.

Experimental Procedure

The apparatus consisted of two smooth-walled, circular, perspex pipes with internal diameters 1 in. and 1 3/4 in. respectively, with orifice diameters 0.375 in. and 0.75 in. respectively. Pressure tappings were formed in the walls of the pipes and a Pitot tube could be traversed at a number of positions. A hypodermic dye injector was used to chart flow patterns and simple U-tube manometers filled with dyed carbon tetrachloride were used throughout for the pressure measurements. In all the experiments the orifices were located at the lowest point of the pipe wall.

Simple visual observations of the orifice leakage formed the first part of the investigation and as expected the issuing jet occupied only a small proportion of the orifice area. The jet was concentrated at the downstream periphery of the orifice and as it left the pipe it had the shape of a curved fan. The angle which the jet axis made with the centreline of the pipe varied with the discharge but was rarely less than 80°.

Pressure velocity measurements were made at each orifice using a range of pipe discharges. Finally, in a restricted series of experiments one pipe was tested with a number of orifices in line, with the pipe outlet open to the atmosphere.

The friction resistance coefficient was determined for the perspex pipes and compared with the Blasius expression

$$c_f = 0.079\, \mathcal{R}^{-1/4} \qquad (19)$$

The experimental value of c_f appeared to be practically constant at a value of 0.0055, and the equivalent range of values using the Blasius expression was 0.0058 to 0.0048.

The results of the other tests are shown in graphical form in figures 3-9.

Figure 3 indicates the relationship between the leakage q and the pipe flow $Q^{7/8}$ for the 1 in. and 1 3/4 in. pipes with the outlet open to atmosphere. A straight line plot is obtained for both pipes indicating that equation 5 is valid although further experimental results should be obtained to confirm this result. The curve relating to the 1 in. pipe shows an apparent departure from a straight line at a value of $Q^{7/8}$ corresponding to a Reynold's number of approximately 2,300 where the flow regime is transitional between turbulent and laminar. The curve for the 1 3/4 in. pipe however departs from a straight line when the Reynold's number is 1.5×10^5 and it would appear that at this value the pipe ceased to "run full" and began to act as a channel with free surface flow. Further, if:

$$\mathcal{R} = 1.5 \times 10^5$$

at the lower end of the straight line the Blasius friction law should not be applied to this flow regime, although the leakage is still evidently proportional to $u^{7/8}$. It is likely that this proportionality would not hold at higher Reynolds' numbers. Another extremely interesting fact is that the orifice discharge for the 3/8 in. orifice in the 1 in. pipe is considerably larger than that issuing from the 3/4 in. orifice in the larger pipe.

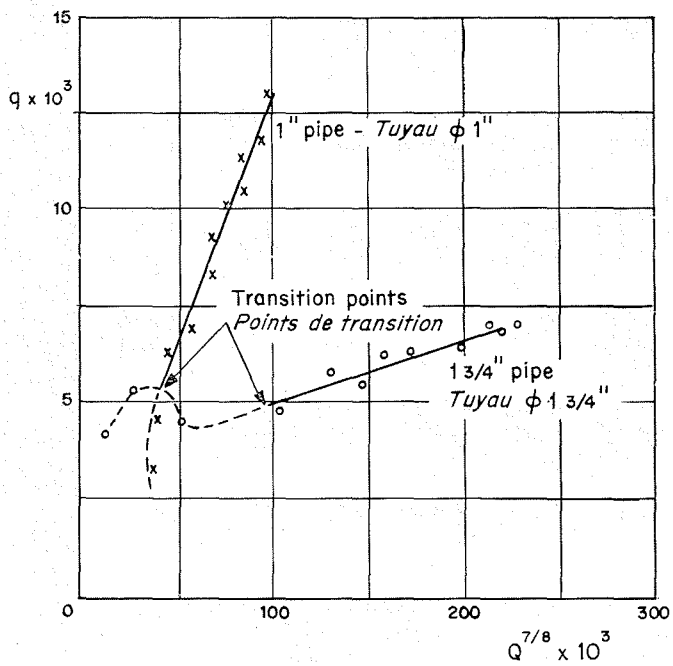

3/ Orifice discharge q plotted against the pipe discharge raised to the seven-eighths power, $Q^{7/8}$.
Débit q *de l'orifice, en fonction du débit du tuyau à la puissance 7/8 :* $q = f(Q^{7/8})$.

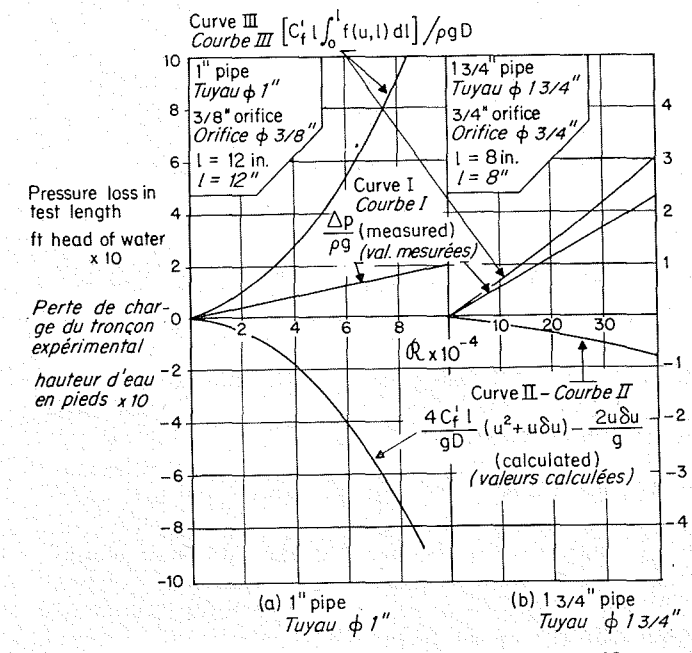

4/ Determination of excess friction loss due to orifice.
Détermination des pertes de charge excédentaires dues au frottement et provoquées par l'orifice.

The values of the coefficient K_1 are 1.31×10^{-3} for the 1 in. pipe and 0.601 for the 1 3/4 in. pipe. A large number of tests are now required to obtain any general expression which would enable K_1 to be determined knowing only the pipe and orifice geometry.

The relationships expressed in equation 18 are plotted in figure 4. Curve (I) represents the measured value of $\sum \Delta p$, i.e. the pressure drop over the test length $2l$, Curve (II) represents the calculated values of

$$2\rho u \{2 c_f l (u + \delta u) - \delta u\}$$

and curve (III) by subtraction of (II) from (I) represents

$$c'_f \frac{l}{D} \int_0^l f(u, l)\, dl$$

each for a range of Reynolds numbers.

The two interesting features in these curves is the very large difference in head loss in the two pipes and the fact that the measured pressure drop is directly proportional to the Reynolds Number.

Static pressure measurement were made at 2 in. intervals upstream and downstream of the orifice. The first set of pressure tappings were in line with the orifice and therefore situated in the lowest part of the periphery of the pipe. The second set were situated in a line on the wall of the pipe and displaced by an angle of 90° from the first set. These tappings were termed the base set and the wall set respectively. The actual values are indicated in Figure 5 for the 1 3/4 in. pipe for a range of discharges. These extremely interesting sets of results provide some of the reasons why some of the apparent anomalies occur when several in-line orifices are tested, Figures 8 and 9.

Reverting to the single orifice, a pressure rise certainly occurs but it cannot yet be stated that the theoretical and practical results agree.

Q (cu. secs)	Predicted pressure rise (ft.)	Measured pressure rise (ft.)
0.158	0.191	0,06
0.130	0.135	0.055
0.102	0.114	0.033
0.055	0.041	0.02

Comparison of measured and calculated values is provided in Table I and the discrepancies are extremely noticeable. However the rise in pressure was measured using tappings 2 in. upstream and downstream of the orifice. For a true comparison the tappings must be placed just upstream and downstream of the orifice.

The pressure variations downstream of the orifice at the base of the pipe, Figure 5 *b* are most marked and probably continue downstream for some distance. It is these pressures that would control the outflow through downstream orifices and this may well account for the fluctuations in discharge shown in Figure 9.

Pitot traverses indicate that these large base pressure fluctuations are confined to a narrow region close to the boundary and that the pressure fluctuations in figure 5 *a* are representative of the general conditions in the pipe.

Velocity profiles in the 1 3/4 in. pipe are shown in Figure 6 for a range of discharges.

It is evident that for both large and small discharges, the kink in the lower portion of the velocity profile develops as the flow progresses downstream. This kinked region also corresponds generally to the area close to the boundary where the pressure fluctuations are greatest.

An impression of a generalised flow pattern is indicated in Figure 7 which is made up from observations of; individual dye streaks provided by the

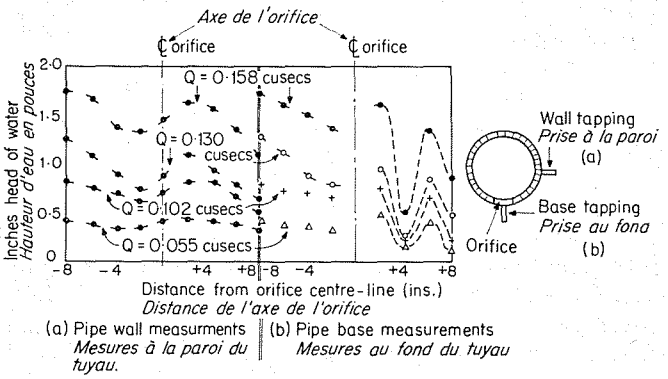

5/ Static pressure measurements at intervals on either side of a 3/4 in. orifice in a 1 3/4 in. perspex pipe. In (*b*) dotted lines are employed downstream of the orifice as an *indication* of the pressure fluctuations.

Mesures de la charge statique, à des distances données de part et d'autre d'un orifice 3/4" dans un tuyau de plexiglas de 1 3/4". Les lignes pointillées, en (b), *sont employées à l'aval de l'orifice à titre* indicatif *des fluctuations de la charge.*

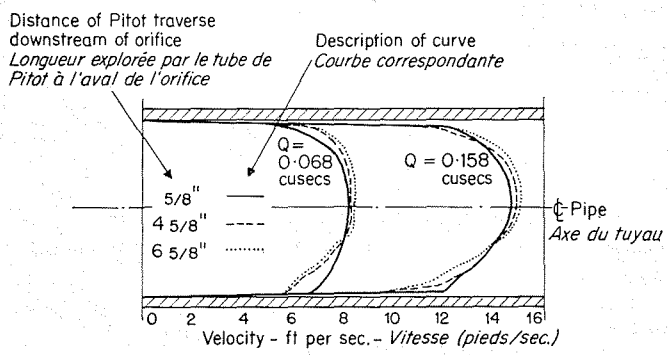

6/ Variation in velocity profile with distance downstream of orifice. 1 3/4 in. pipe, 3/4 in. orifice.

Variation des profils de vitesse en fonction de la distance à l'aval de l'orifice. Tuyau de 1 3/4", orifice de 3/4".

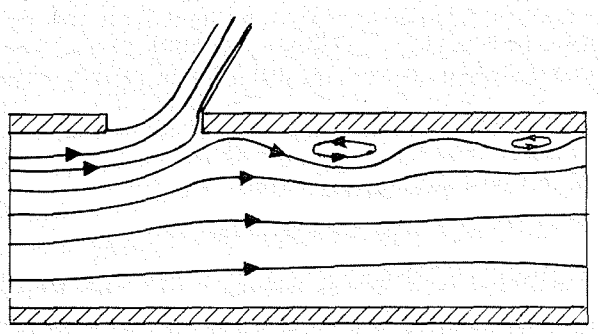

7/ Generalised view of flow patterns in the vicinity of an orifice.

Aspect généralisé du schéma d'écoulement au voisinage d'un orifice.

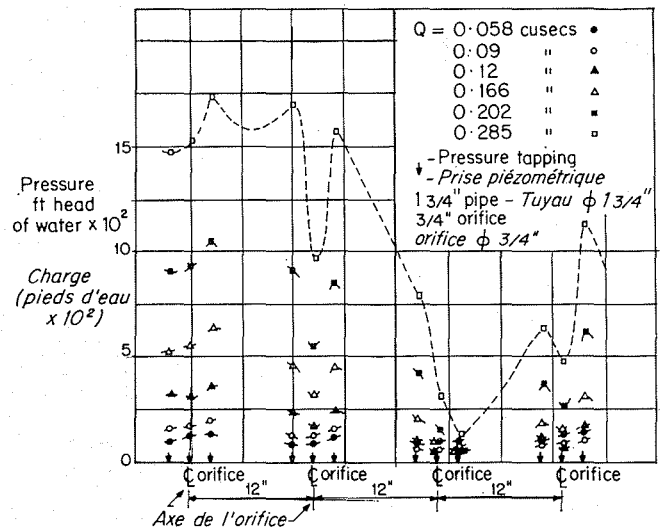

8/ Static pressures measured 2 in. upstream and downstream of 4 in—line orifices, spaced at 12 in. centres. For ease of viewing one set of measurements (Q = 0.285 cusecs) are joined by a dotted line. It is understood however that pressures between the tapping points may not correspond to this curve.

Charges statiques mesurées à 2" à l'amont et à l'aval de 4 orifices alignés, à 12" d'entre-axes. La ligne discontinue reliant les points correspondant à un ensemble de mesures a été ajoutée pour clarifier la représentation (Q = 0,285 cusecs) mais il est entendu que les charges existant entre les points de mesure ne correspondent pas forcément à cette ligne.

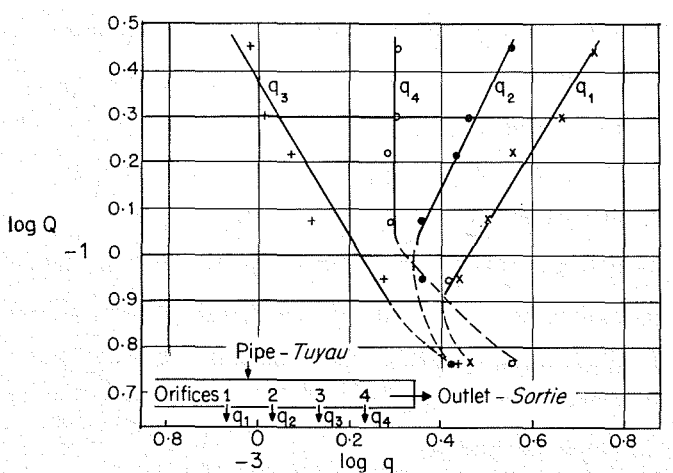

9/ Plotting Q/q logarithmically for four in-line orifices. It would appear that for values of log Q > T.10 the relationship is linear, i.e. log Q = *m* log *q* + C.

Graphique, en coordonnées logarithmiques, des rapports Q/q correspondant à 4 orifices alignés. La relation paraît linéaire pour les valeurs de log Q > T.10, de sorte que log Q = m log q + C.

hypodermic dye injector. It is clear that only a small fraction of the area of the orifice is used by the outflowing jet and that the flow downstream separates from the boundary leaving a vortex region. A second but smaller vorted is formed further downstream and it is likely that even more are formed even further downstream. These vortex areas probably coincide with the high pressure areas at the base of the channel shown in Figure 5.

Conclusions

Evidently this investigation leaves many questions unanswered but it is of value in laying the ground for work for a more complete analysis which, however, would have to deal with a number of aspects of the problem:—

The value of K_1, the orifice discharge coefficient, must be determined for a variety of pipe and orifice diameters and then codified in order that it may be predicted. Similarly K_2 the orifice pressure rise coefficient must be determined and the related coefficient K_3 and K_4 for the laminar flow range.

The determination of the excess friction factor c_f is also of considerable importance and in particular of the explicit form of the function $f(u, l)$, i.e. how this loss is related to the mean velocity and to the distance downstream of the orifice.

Whilst these investigations will be of value, it is realised that they are merely a prelude to the wider problem of orifices in line and possible to the problem of multiple orifices in a pipe wall. Further a useful extension of this work would be to consider similar geometric arrangements but with the pipe outlet blocked.

The pressure variations and orifice discharges for the 1 3/4" pipe with three orifices situated downstream of the first orifice at 12 in. as are shown in Figures 8 and 9. There is some evidence of a connected pattern of cause and effect but a much more intensive investigation is required before this matter can be discussed in detail. It is sufficient to note that although in general a pressure rise (predicted theoretically) occurs across the upstream orifice, this rise does not always occur across the other orifices. Further, the general pattern of a decreasing pressure along the length of the pipe no longer holds and the discharge from the orifices appears to vary in a most arbitrary manner. Evidently the leakage through succeeding orifices is considerably affected by that in the preceeding ones. It is noteworthy that the lowest pressure occurs at orifice number 3 and this orifice provides the smallest discharges.

Finally one simple but extremely interesting test showed that air can be sucked into the pipe through the orifice. A naked flame held near the orifice indicated this and the result was confirmed by cutting a small mask that covered all that part of the orifice not discharging water. The measured head loss, over a test length, was increased by a small but relatively consistent amount when the mask was in place indicating that a change in flow had occurred and the only change could be the cessation of the influx of air into the pipe.

Résumé

L'écoulement par un orifice plan dans la paroi d'une conduite

par
J. A. Sandover *
et
J. A. Tallis **

Il est possible de démontrer tant théoriquement que par voie expérimentale que la charge augmente à travers un orifice plan dans la paroi d'une conduite débitant en charge. On peut montrer, également, que l'énergie totale décroît à travers ce même orifice.

Il ressort de la figure 1, et des équations 1, 2, et 3, que le débit théorique par l'orifice est donné par l'équation 5 :

$$q = K_1 u^{7/8}$$

dans laquelle, d'après l'équation 4, la valeur de K_1 est égale à :

$$K_1 = 0{,}443\ C_D d^2 L^{1/2} \nu^{1/8} / D^{5/8}$$

laquelle peut être déterminée par voie expérimentale.

L'application de l'équation de la quantité de mouvement (6) au tronçon délimité par les sections 1 et 2, permet la représentation de l'augmentation de charge par l'équation 7, et, à l'aide des équations 8 (de continuité) et 4, cette équation 7 peut alors s'écrire sous forme de l'équation 10 :

$$p_2 - p_1 = K_2 u^{15/8}$$

avec (équation 9) $K_2 = 1{,}128\ C_D d^2 L^{1/2} \nu^{1/8} / D^{21/8}$.

La valeur de K_2 peut être déterminée par voie expérimentale. De même, K_3 et K_4 (équations 12 et 14) ont trait au régime laminaire.

Il avait toutefois été tenu compte, pour l'expérience initiale, de la perte de charge Δp sur des longueurs l à l'amont et l à l'aval de l'orifice. La considération du deuxième membre de l'équation 17, et de la figure 2 permet d'expliquer les anomalies apparentes constatées. Le premier terme (courbe A) représente la perte de charge normale; l'augmentation de la charge (courbe B) à travers l'orifice est représentée par le troisième terme; la courbe C, enfin, est indiquée par le deuxième terme représentant la perte de charge correspondant à la longueur aval, et étant équivalente à celle représentée, pour la longueur l amont, par la courbe A. Le quatrième terme est égal à Δp sur le schéma, étant représenté par la courbe D, soit la répartition réelle des charges à l'aval. Le coefficient de rugosité c'_f correspondant à cette longueur est une fonction qui dépend probablement du nombre de Reynolds de l'écoulement. Les facteurs c'_f et $f\ (u, l)$ demandent une étude poussée.

Les valeurs globales de Δp peuvent être déterminées par voie expérimentale (étant donné la possibilité d'évaluer les autres termes des équations 17 et 18), et sont indiquées en figure 4.

Bien que la pression augmente à travers l'orifice, il est nécessaire de démontrer que l'énergie globale décroît; la valeur de cette décroissance ΔH s'obtient expérimentalement à partir de l'équation 16.

Ensuite, la substitution de cette valeur de ΔH dans l'équation 15 permet d'évaluer c'_f et $f\ (u, l)$, et de comparer les résultats ainsi obtenus avec ceux fournis par l'équation 18.

L'expérience a été effectuée à l'aide de deux conduites en plexiglas aux parois épaisses, présentant des diamètres, respectivement, de 2,54 cm et de 4,44 cm, et comportant, le premier un orifice de 0,95 cm, et le deuxième un orifice de 1,9 cm. Après un examen visuel des caractéristiques de l'écoulement, il a été procédé à la mesure des débits, q par l'orifice, et Q par la conduite; ces résultats sont représentés par la figure 1, et indiquent la validité de l'équation 5.

Les valeurs des charges statiques au fond et aux parois latérales de la conduite sont indiquées par la figure 5. Les écarts constatés entre les valeurs théoriques et expérimentales des « gains » de pression à travers les orifices sont donnés par le tableau I, mais il sera nécessaire de revérifier ces résultats au moyen de mesures à l'aide de prises de pression situées juste à l'amont et juste à l'aval de l'orifice.

Les profils de répartition des vitesses obtenues par exploration au tube de Pitot sont indiqués sur la figure 6, correspondant à deux débits, et à trois distances différentes à l'aval d'un orifice. Le schéma d'écoulement généralisé, obtenu à l'aide de ces résultats et d'injections de filets de colorant par une seringue hypodermique, est représenté par la figure 7. Les figures 8 et 9 sont relatives à des expériences préliminaires réalisées avec une seule conduite comportant 4 orifices alignés.

Conclusion. — Cette étude est une étude préliminaire. Pour le cas d'orifices simples, il est nécessaire de déterminer les coefficients K_1 à K_4, et d'étudier le coefficient de rugosité équivalente c'_f et le facteur $f\ (u, l)$. La présente étude a toutefois permis de résoudre certaines anomalies apparentes, et pourra sans doute servir de point de départ utile pour les études futures.

---

* Ph. D.
** B. Sc.